

# SCIENTIFIC REPORTS



OPEN

## Secondary batteries with multivalent ions for energy storage

Chengjun Xu<sup>1</sup>, Yanyi Chen<sup>1</sup>, Shan Shi<sup>1,2</sup>, Jia Li<sup>1</sup>, Feiyu Kang<sup>1,2</sup> & Dangsheng Su<sup>3,4</sup>

Received: 18 November 2014

Accepted: 21 July 2015

Published: 14 September 2015

The use of electricity generated from clean and renewable sources, such as water, wind, or sunlight, requires efficiently distributed electrical energy storage by high-power and high-energy secondary batteries using abundant, low-cost materials in sustainable processes. American Science Policy Reports state that the next-generation “beyond-lithium” battery chemistry is one feasible solution for such goals. Here we discover new “multivalent ion” battery chemistry beyond lithium battery chemistry. Through theoretic calculation and experiment confirmation, stable thermodynamics and fast kinetics are presented during the storage of multivalent ions ( $\text{Ni}^{2+}$ ,  $\text{Zn}^{2+}$ ,  $\text{Mg}^{2+}$ ,  $\text{Ca}^{2+}$ ,  $\text{Ba}^{2+}$ , or  $\text{La}^{3+}$  ions) in alpha type manganese dioxide. Apart from zinc ion battery, we further use multivalent  $\text{Ni}^{2+}$  ion to invent another rechargeable battery, named as nickel ion battery for the first time. The nickel ion battery generally uses an alpha type manganese dioxide cathode, an electrolyte containing  $\text{Ni}^{2+}$  ions, and Ni anode. The nickel ion battery delivers a high energy density ( $340\text{Wh kg}^{-1}$ , close to lithium ion batteries), fast charge ability (1 minute), and long cycle life (over 2200 times).

The use of electricity generated from clean and renewable sources, such as water, wind, or sunlight, requires efficient distributed electrical energy storage by high-power and high-energy secondary batteries using abundant, low-cost materials in sustainable processes<sup>1</sup>. The secondary batteries capable of storing enormous electric energy at a very large power are of importance for our society. Battery, whose chemistry is based on cathodic and anodic reactions occurring at the interface between the electrodes and electrolyte, generally composes of a cathode, an anode, an electrolyte and a separator<sup>2</sup>. Secondary battery is rare in battery industries because it is difficult to gather two electrochemically reversible cathodic and anodic reactions in one electrolyte as the battery chemistry. There are only several kinds of secondary (rechargeable) batteries in the world: lithium, lithium ion (LIB), sodium ion, nickel cadmium (Ni-Cd), lead-acid, magnesium, calcium and aluminum batteries<sup>1,3–12</sup>. Most of the current batteries, for example lithium ion batteries, utilize univalent ions (i.e.  $\text{H}^+$ ,  $\text{Li}^+$ ,  $\text{Na}^+$  or  $\text{K}^+$ ) as media to store energy. Moreover, most of them are incapable of fast charge<sup>8,13</sup>. Here, we show “how to discover the secondary battery chemistry with the multivalent ions for energy storage” and report a new rechargeable nickel ion battery with fast charge rate. There are three steps for the fabrication of a battery. Firstly, we need choose two reversible reactions in one electrolyte as the cathodic and anodic reactions, respectively. Secondly, suitable cathode and anode materials are required to carry out these reactions. Finally the rechargeable battery is fabricated with certain cathode, anode, electrolyte, and a separator.

The multivalent ions, for example  $\text{Mg}^{2+}$  or  $\text{Al}^{3+}$  ion, are used for energy storage to fabricate magnesium or aluminum battery<sup>10–12,14–17</sup>. The investigation on the reversible intercalation of  $\text{Mg}^{2+}$  ions into Chevrel phase such as  $\text{Mo}_3\text{S}_4$  indicated an extremely slow intercalation kinetics and low charge capacity<sup>17</sup>. It is generally believed that the kinetics of insertion of multivalent ions into host solid state electrode is much slower than that of univalent ions. While in  $\text{MnO}_2$ -based supercapacitors the charge rate and capacitance of the host electrode material (for example  $\text{MnO}_2$ ) can be doubled by using multivalent  $\text{Ca}^{2+}$

<sup>1</sup>Graduate School at Shenzhen, Tsinghua University, Shenzhen 518055, P. R. China. <sup>2</sup>State Key Laboratory of New Ceramics and Fine Processing, Department of Materials Science and Engineering, Tsinghua University, Beijing 100084, P. R. China. <sup>3</sup>Department of Inorganic Chemistry, Fritz Haber Institute of the Max Planck Society, Faradayweg 4–6, 14195 Berlin, Germany. <sup>4</sup>Shenyang National Laboratory of Materials Science, Institute of Metal Research, Chinese Academy of Sciences, Shenyang 110016, P. R. China. Correspondence and requests for materials should be addressed to C.X. (email: vivaxuchengjun@163.com)

Species	Diameter (Å)	$D_0$ ( $\times 10^{-14} \text{m}^{-2} \text{s}^{-1}$ )	$nD_0$ ( $\times 10^{-14} \text{m}^{-2} \text{s}^{-1}$ )	$\Delta E$ (eV)	Storage capacity ( $\text{mAh g}^{-1}$ )
$\text{Li}^+$	0.69	13.8	13.8	-5.006	63
$\text{Na}^+$	1.02	11.6	11.6	-4.493	68
$\text{K}^+$	1.38	7.3	7.3	-4.463	53
$\text{Mg}^{2+}$	0.66	11.4	22.8	-5.601	97
$\text{Ca}^{2+}$	0.99	9.8	19.6	-7.282	99
$\text{Ba}^{2+}$	1.34	6.9	13.8	-7.308	81
$\text{Zn}^{2+}$	0.74	4.3	8.6	-2.092	220
$\text{Ni}^{2+}$	0.72	7.5	15.0	-5.54	298
$\text{La}^{3+}$	1.06	3.7	11.1	-10.019	101

**Table 1.** Detailed information of univalent and multivalent ions.

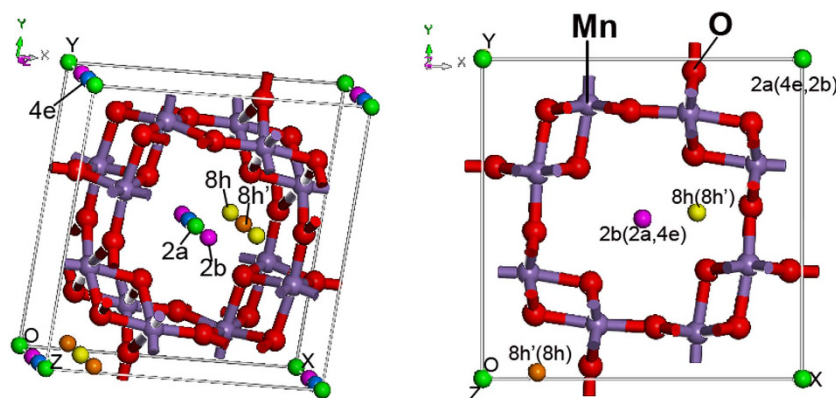


**Figure 1.** Possible positions (2a, 2b, 4e, 8h' and 8h) in the tunnel of  $\alpha\text{-MnO}_2$  for the insertion of univalent and multivalent ions. (The pictures are drawn by C. Xu and S. Shi).

ion compared with univalent  $\text{Na}^+$  ion<sup>18–24</sup>. By using trivalent  $\text{La}^{3+}$  ion, the charge rate and capacitance of  $\text{MnO}_2$  can be further improved<sup>22</sup>. The research in the supercapacitor application inspired us that we can set up suitable systems for multivalent ions to obtain high intercalation capacity and a fast charge rate. We absorbed the idea and use it in battery field to invent rechargeable batteries with high energy density and fast charge rate. We realized this idea by using the insertion of multivalent  $\text{Zn}^{2+}$  or  $\text{Ni}^{2+}$  ion into alpha type manganese dioxide to invent two rechargeable batteries with a very fast charge rate<sup>23</sup>. In this manuscript, we report the energetic nickel ion chemistry and nickel ion battery for the first time. The nickel ion battery generally uses an alpha type manganese dioxide cathode, an aqueous  $\text{NiSO}_4$  electrolyte, and Ni anode. The nickel ion battery displays a high energy density ( $340 \text{ Wh kg}^{-1}$ , close to that of lithium ion batteries), fast charge ability (1 minute) and long cycle life (over 2200 times).

## Results

The common view that the multivalent ion is unsuitable for energy storage at a fast rate is not correct. Below we show that the storage of multivalent ions in certain host material with a large tunnel structure is feasible both thermodynamically and kinetically. Table 1 shows that the ion dynamic diameters of the multivalent ions are close to that of the univalent ions. It enables the probability of multivalent ions to be stored in alpha type manganese dioxide ( $\alpha\text{-MnO}_2$ ) with a tunnel diameter of 0.28 nm.

We simulated the insertion of one ion in several possible positions (such as 2a, 2b, 4e, 8h' and 8h) of one  $\alpha\text{-MnO}_2$  tunnel by first principle calculation (Fig. 1)<sup>9,25</sup>. The summary of  $\text{Li}^+$ ,  $\text{Na}^+$ ,  $\text{K}^+$ ,  $\text{Ni}^{2+}$ ,  $\text{Zn}^{2+}$ ,  $\text{Mg}^{2+}$ ,  $\text{Ca}^{2+}$ ,  $\text{Ba}^{2+}$ , or  $\text{La}^{3+}$  ion inserting in various positions can be seen in Table S1. The  $\text{Li}^+$ ,  $\text{Na}^+$ ,  $\text{Zn}^{2+}$ ,  $\text{Mg}^{2+}$ , and  $\text{Ca}^{2+}$  ions favour inserting in the 8h position of the tunnel, while  $\text{Ni}^{2+}$  ion favour the 2a position and  $\text{K}^+$ ,  $\text{Ba}^{2+}$  and  $\text{La}^{3+}$  ions favour the 2b position. The bond length of A–O ranges from 1.83 to 2.89 Å for different ion species (Table S1). When an ion inserts into the tunnel of  $\alpha\text{-MnO}_2$ , the tunnel slightly changes and the electrons are stored and shared by adjacent Mn and O atoms. The lowest binding energy ( $\Delta E$ ) after ion-insertion for each ion is listed in Table 1. The lower binding energy of multivalent “ion-insertion” indicates that insertion of multivalent ions is thermodynamically easier and more stable than insertion of univalent ions<sup>9,25</sup>.

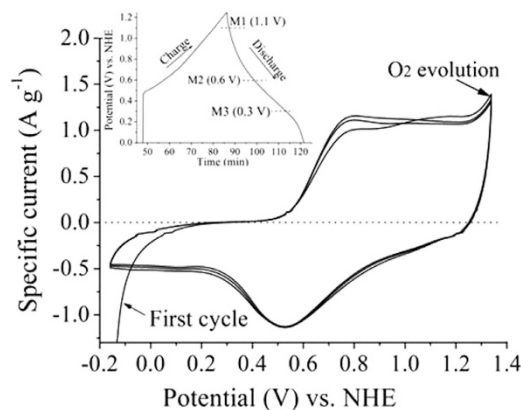
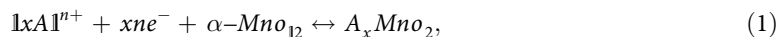


**Figure 2.** Cyclic voltammetric curve of  $\alpha$ - $\text{MnO}_2$  electrode at a sweep rate of 1 millivolt per second in  $1.0 \text{ mol L}^{-1}$   $\text{NiSO}_4$  electrolyte. The insert shows the charge/discharge curve of  $\alpha$ - $\text{MnO}_2$  electrode in  $1.0 \text{ mol L}^{-1}$   $\text{NiSO}_4$  electrolyte at a current density of 0.2 Ampere per gram.

Moreover, the kinetics of charge rate by using multivalent ion is faster than using univalent ion, which is directly seen as  $nD_0$  in Table 1.  $D_0$  represents the diffusion coefficient and  $n$  is the valence state of these cations. Most importantly, compared with univalent ion, the multivalent ions have the advantage that each multivalent ion inserting into  $\alpha$ - $\text{MnO}_2$  host results in the charge storage of over one electron (Figure S6). The lower required energy and faster charge rate of multivalent ions inserted into  $\alpha$ - $\text{MnO}_2$  enable the high capacity and fast charge ability for energy storage, which is also consistent with the experimental results in literature<sup>18,20–23</sup>.

In the first time, we experimentally found that each multivalent  $\text{Ni}^{2+}$ ,  $\text{Zn}^{2+}$ ,  $\text{Mg}^{2+}$ ,  $\text{Ca}^{2+}$ , and  $\text{Ba}^{2+}$  ion can electrochemically insert/extract into/from the tunnels of  $\alpha$ - $\text{MnO}_2$  as cathodic reaction.



where  $\text{A}^{n+}$  represents  $\text{Ni}^{2+}$ ,  $\text{Zn}^{2+}$ ,  $\text{Mg}^{2+}$ ,  $\text{Ca}^{2+}$ ,  $\text{Ba}^{2+}$ , or  $\text{La}^{3+}$  ion and  $n$  is the charge number<sup>18,20–23</sup>. The electrolyte refers to the aqueous solution of each multivalent ion with pH value ranging from 4.0 to 7.0, for example 1 mole per liter ( $\text{mol L}^{-1}$ )  $\text{Ba}(\text{NO}_3)_2$  or  $\text{NiSO}_4$  aqueous solution. Figure 2 shows the storage of each multivalent ion in  $\alpha$ - $\text{MnO}_2$ . It can be seen that  $\text{Ni}^{2+}$  ion can insert/extract into/from  $\alpha$ - $\text{MnO}_2$  within a potential window ranging from 0.2 to 1.3 V (vs. NHE) reversibly. Insert of Fig. 2 shows the charge/discharge curves of reversible insertion/extraction of  $\text{Ni}^{2+}$  ion into/from  $\alpha$ - $\text{MnO}_2$ . The results regarded to  $\text{Zn}^{2+}$ ,  $\text{Mg}^{2+}$ ,  $\text{Ca}^{2+}$ ,  $\text{Ba}^{2+}$ , or  $\text{La}^{3+}$  ion have already been published and showed that the capacitance and charge rate of  $\alpha$ - $\text{MnO}_2$  could significantly double when replacing univalent  $\text{Li}^+$ ,  $\text{Na}^+$ , or  $\text{K}^+$  ion with them<sup>18–23</sup>. In this paper, the fast reversible insertion/extraction of  $\text{Ni}^{2+}$  ion into/from  $\alpha$ - $\text{MnO}_2$  is firstly investigated. Most importantly, we use multivalent  $\text{Ni}^{2+}$  ion to invent a new rechargeable battery, named as nickel ion battery. Apart from  $\alpha$ - $\text{MnO}_2$ ,  $\text{MnO}_2$  samples with other typical tunnel structures, for instance,  $\beta$ - $\text{MnO}_2$ ,  $\gamma$ - $\text{MnO}_2$  and  $\delta$ - $\text{MnO}_2$ , are also explored to store  $\text{Ni}^{2+}$  (See Part 1 in SI). However, a reversible intercalation process of  $\text{Ni}^{2+}$  ions only occurs in  $\alpha$ - $\text{MnO}_2$  due to its large and unique tunnel structure.

We further confirmed the storage of  $\text{Ni}^{2+}$  ions into  $\alpha$ - $\text{MnO}_2$  by X-ray photoelectron spectroscopy (XPS) and element mapping measurements. In order to explore the storage of  $\text{Ni}^{2+}$  ions into  $\alpha$ - $\text{MnO}_2$ , individual  $\alpha$ - $\text{MnO}_2$  electrode is discharged from 1.25 to 1.1, 0.6, 0.3 V (denoted as M1, M2, and M3) by XPS and element mapping measurements, respectively. XPS analysis on the M1, M2, and M3 electrodes is employed to monitor the valence change of Mn and the molar ratio between nickel and manganese element after discharging (See part 2 in SI). The XPS survey of M1, M2 and M3 electrodes is shown in Fig. 3a. Figure 3b exhibits the Mn 3s core levels for as-prepared, M1, M2, and M3 electrodes. The difference values of peak energies of the Mn 3s are 5.08, 5.10, 5.32 and 5.43 eV for as-prepared, M1, M2, and M3 electrodes, respectively. These values are compared to 5.79, 5.50, 5.41, and 4.78 eV for reference samples of  $\text{MnO}$ ,  $\text{Mn}_3\text{O}_4$ ,  $\text{Mn}_2\text{O}_3$ , and  $\text{MnO}_2$ , respectively<sup>9,23</sup>. A clear change of peak splitting of Mn 3s was obtained during discharging, which indicates that the oxidation state of manganese changed from IV in oxidized state to III in reduced state. This plot shows that the average valence state of Mn decreased when the  $\text{MnO}_2$  electrode discharged, which means that a part of  $\text{Mn(IV)}$  ions is reduced to  $\text{Mn(III)}$  ion and the energy (electrons) is stored. Moreover, the oxidation state of  $\alpha$ - $\text{MnO}_2$  is almost the same after charge/discharge.

The Ni 3p and Ni 2p core level spectra of M1, M2 and M3 electrodes are shown in Fig. 4. As the potential decreases the molar ratio between Ni and Mn increases from 0.00 to 0.19, which clearly indicates the storage of  $\text{Ni}^{2+}$  ion in  $\alpha$ - $\text{MnO}_2$ . The transmission electron microscope (TEM) mapping results of M1, M2, and M3 electrodes are shown in Fig. 5. It can be seen that the morphology of the  $\alpha$ - $\text{MnO}_2$

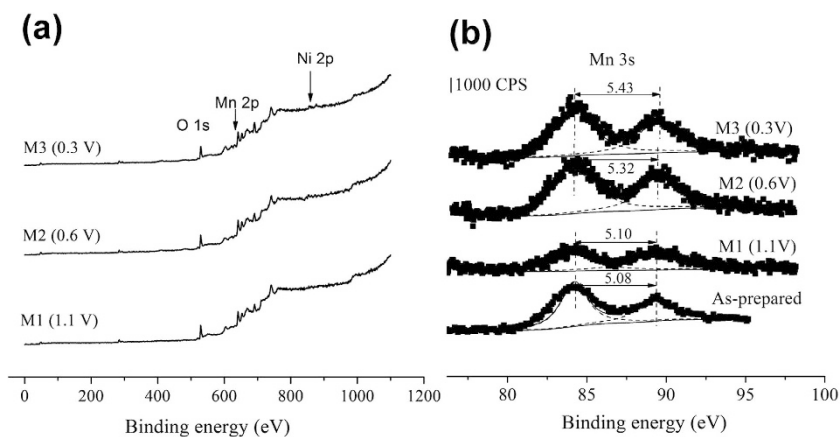


**Figure 3.** (a) The XPS survey of M1, M2 and M3 electrodes. (b) The Mn 3s core level spectra of as-prepared, M1, M2 and M3 electrodes.

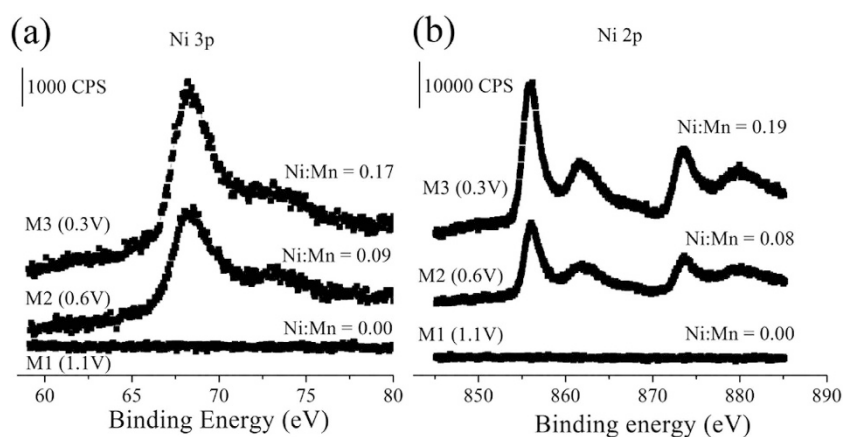


**Figure 4.** (a) Ni 3p and (b) Ni 2p core level spectra of M1, M2 and M3 electrodes.

sample synthesized by the co-precipitation technique is rod-like shape with tens of nanometers in diameter. During discharging process, the electrode Ni ions are stored in  $\text{MnO}_2$ . Therefore, results from XPS and TEM element mapping measurement directly demonstrated that  $\text{Ni}^{2+}$  ions are stored in  $\alpha\text{-MnO}_2$ . Furthermore, X-ray diffraction (XRD) measurement is used to monitor the structure change of  $\text{MnO}_2$  during the storage process of  $\text{Ni}^{2+}$  ions. It suggests that the main infrastructure of  $\text{MnO}_2$  has not been changed dramatically with the insertion of  $\text{Ni}^{2+}$  ions (Figure S7).

## Discussion

Generally, a battery composes of a cathode, an anode, an electrolyte and a separator. And battery chemistry is based on cathodic and anodic reactions occurring at the interface between electrode and electrolyte. We firstly discover the fast reversible insertion/extraction of  $\text{Ni}^{2+}$  ion into/from  $\alpha\text{-MnO}_2$  in  $1 \text{ mol L}^{-1}$   $\text{NiSO}_4$  aqueous solution as shown in equation 2. Therefore, the  $\alpha\text{-MnO}_2$  electrode and  $1 \text{ mol L}^{-1}$   $\text{NiSO}_4$  aqueous solution can be used as the cathode and the electrolyte, respectively. It also indicates that the reaction of equation 1 can be the cathodic reaction. Then reliable anode as well as anodic reaction has to be found for each multivalent ion to fabricate a full battery. Metal anode is the typical anode used in secondary battery chemistry. In the aqueous electrolyte, Ni metal is suitable for the anode. Deposition/dissolution of  $\text{Ni}^{2+}/\text{Ni}$  occurs at ca.  $-0.23 \text{ V}$  vs. NHE in  $1 \text{ mol L}^{-1}$   $\text{NiSO}_4$  aqueous electrolyte (red line in Fig. 6a). The deposition of  $\text{Ni}^{2+}$  ion on Ni metal is found to be spherical shape with tens of nanometers in diameter (Figure S8).

With the  $\alpha\text{-MnO}_2$  as cathode, Ni metal as anode, and  $1 \text{ mol L}^{-1}$   $\text{NiSO}_4$  aqueous solution as electrolyte, we can invent a rechargeable battery. The battery chemistry is based on two electrochemically reversible cathodic and anodic reactions (equation 2 and equation 3). The potential ranges of cathodic reaction and anodic reaction are showed in Fig. 6a.



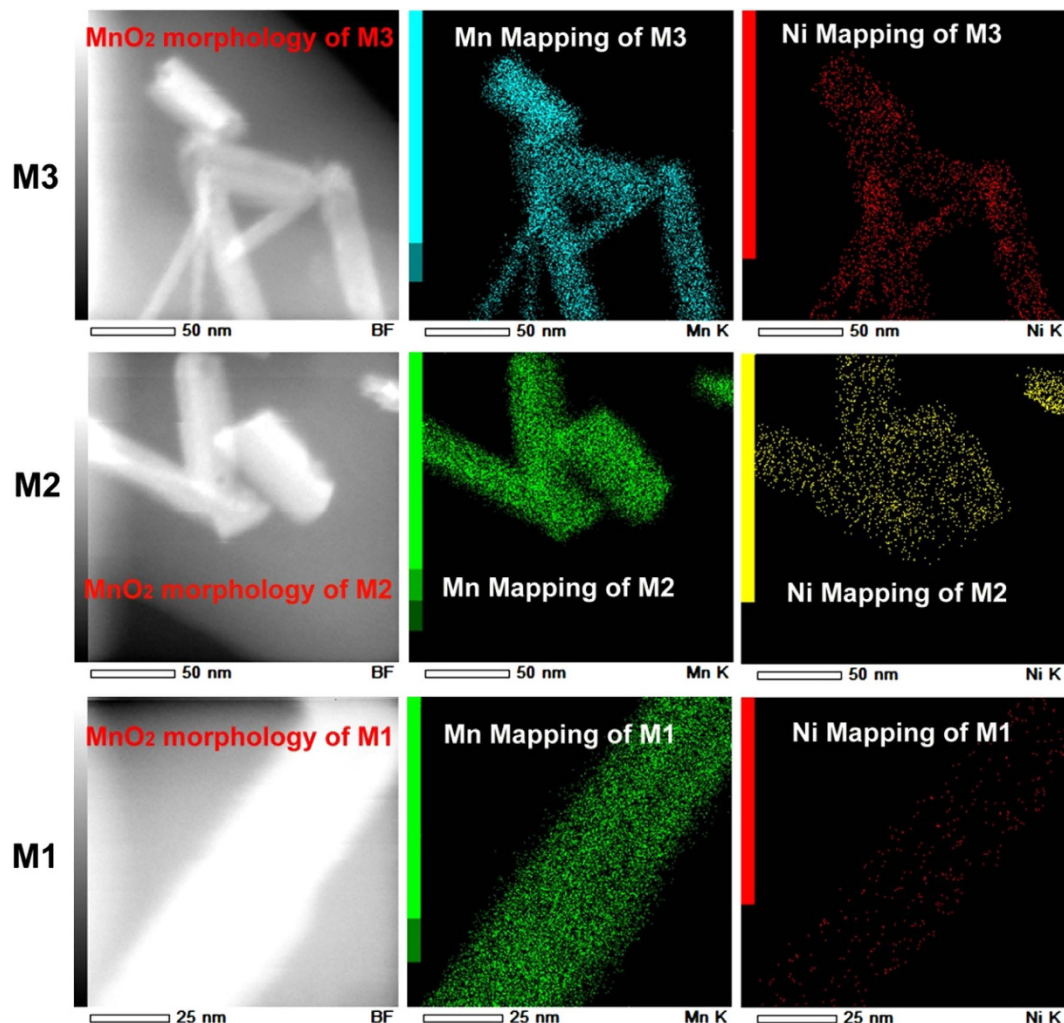


**Figure 5.** The morphology, Mn element mapping, and Ni element mapping of MnO<sub>2</sub> in M1, M2, and M3 electrodes.

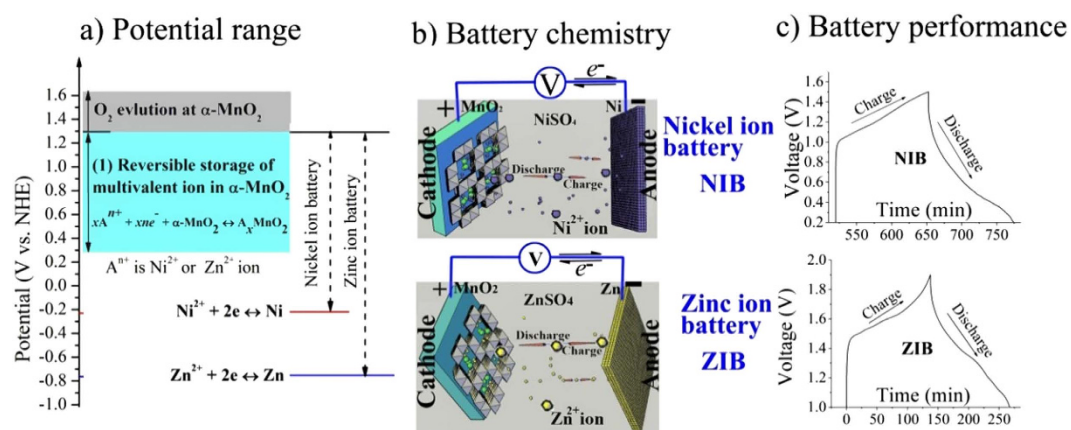


**Figure 6.** (a) The potential ranges of equations 2 to 3 (Solid lines). The dash lines show the maximum operating voltage of nickel ion battery (NIB) and zinc ion battery (ZIB). (b) The energetic chemistry of NIB and ZIB. NIB or ZIB use Ni<sup>2+</sup> or Zn<sup>2+</sup> ion as storage in both α-MnO<sub>2</sub> cathode and Ni or Zn metal anode, respectively. (c) The charge/discharge curves of NIB and ZIB. This plot also shows the three steps to invent a rechargeable battery. (The pictures are drawn by C. Xu and S. Shi).

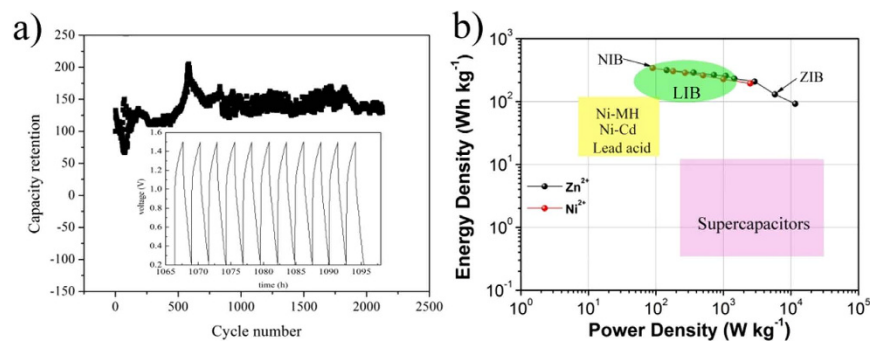
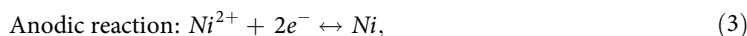
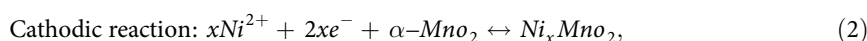


**Figure 7.** (a) Long cycle life of nickel ion battery at current density of 0.2 Ampere per gram. Inserts shows the charge/discharge curves of nickel ion battery. (b) Ragone plots of nickel ion battery (NIB) and zinc ion battery (ZIB) marked with line with dots, compared with state-of-the-art lead acid battery (Lead Acid), nickel cadmium (Ni-Cd), lithium ion battery (LIB) and supercapacitors marked with colorful area.



Subsequently, the energetic nickel ion chemistry as shown in Fig. 6b is proposed by using  $\text{Ni}^{2+}$  ion as the energy storage medium. Nickel ion battery composes of an  $\alpha\text{-MnO}_2$  cathode, a nickel metal anode, and a  $\text{NiSO}_4$  mild aqueous electrolyte. During discharging process, anodic nickel is dissolved in the form of  $\text{Ni}^{2+}$  ion, which then inserts into  $\alpha\text{-MnO}_2$  cathode, generating an electron current flow in the electrical loop and vice versa. Because the storage/release of energy is based on the migration of  $\text{Ni}^{2+}$  ion between cathode and anode, we name this battery as nickel ion battery (NIB).

In addition, Fig. 6 also shows the information of zinc ion battery (ZIB) to compare with NIB. ZIB is assembled by using  $\alpha\text{-MnO}_2$  cathode, Zn anode and  $\text{ZnSO}_4$  aqueous electrolyte<sup>23</sup>. It can be seen from Fig. 6 that NIB and ZIB are similar in cathode due to the origin of the multivalent ion storage mechanism of  $\alpha\text{-MnO}_2$ . However, the electrolyte, anode and the most important battery chemistry are different.

We assembled the prototype NIB (See Part 4 in SI) and ZIB (See Part 5 in SI), whose charge/discharge curves are shown in Fig. 6c. The NIB has a maximum operating voltage value of 1.5 V and delivers a capacity up to 298 milliamper hour per gram ( $\text{mAh g}^{-1}$ ) calculated based on the mass of  $\text{MnO}_2$ . The long cycle life test has been performed on NIBs by the continuous galvanostatic charge/discharge at current densities of 200 milliamper per gram as shown in Fig. 7a. The continuous charge/discharge cycle curves of NIB are showed in the insert of Fig. 7a. After 2200 cycles NIB still shows a stable capacity and good columbic efficiency (Figure S13). The Ragone plots of NIB and ZIB are shown in Fig. 7b. It exhibits that these energy storage devices with multivalent  $\text{Zn}^{2+}$  or  $\text{Ni}^{2+}$  ions for energy storage cover a very wide range from batteries to supercapacitors and fill the gap between them.

Batteries with the multivalent ions for energy storage, for example NIB and ZIB, are capable of fast charge/discharge (1 minute) as shown in the insert of Fig. 7a and Figure S15. The energy densities of ZIB and NIB are estimated to be ca. 320 and 340 watt hours per kilogram ( $\text{Wh kg}^{-1}$ ) based on the weight of the total active mass of both cathode and anode. In the battery industry, the weight of the active mass of both cathode and anode is 30–50% of the total battery<sup>13</sup>. Therefore, the energy densities of total battery of ZIB and NIB should be up to 170  $\text{Wh Kg}^{-1}$  and ca. 120  $\text{Wh Kg}^{-1}$ , which are higher than lead-acid, or Ni-Cd batteries (ca. 40–80  $\text{Wh kg}^{-1}$ ), and close to LIB (ca. 150–400  $\text{Wh kg}^{-1}$ )<sup>2,9,13,26–29</sup>. In addition, NIB shows a longer cycle life over 2200 cycles than current aqueous batteries (ca. 1000 cycles)<sup>2,30</sup>. Furthermore, we have performed the nailing experiment on these batteries at a fully charged state. No sign of flash or smoke has been detected, which indicates the excellent safety. Therefore, these secondary batteries have great advantages in terms of safety, cycle life and energy density over the existing rechargeable batteries. These significant advantages enable the exploration of new industrial applications or to rival lead-acid or nickel cadmium batteries. For example, these secondary batteries are advanced candidates for hybrid electric vehicles or electric bicycles, or for storage of electricity generated from clean and renewable sources, such as water, wind or sunlight. This is just the beginning of searching for new batteries with multivalent ions. With the further exploration we anticipate that more rechargeable batteries with multivalent ions as energy storage will emerge.

In summary, we show that storage of multivalent  $\text{Ni}^{2+}$  or  $\text{Zn}^{2+}$  ion in alpha type manganese dioxide presents a stable thermodynamics and fast kinetics, which is confirmed by theoretic calculation and experiment confirmation. We further use storage process of the multivalent  $\text{Ni}^{2+}$  ions to discover a new battery chemistry and invent the rechargeable nickel ion battery. The secondary battery with multivalent

Ni<sup>2+</sup> ions for energy storage is advantageous in energy density (340 Wh kg<sup>-1</sup>), fast charge ability (1 minute), and long cycle life (over 2200 times). As multivalent ions are rich in quantity, we believe that the utilization of them may trigger a renaissance of new battery chemistry in the future.

## Methods

The MnO<sub>2</sub> powder has been synthesized by a one step process or co-precipitation technique<sup>19</sup> (See Methods in SI). Electrodes were prepared by mixing 70 wt% of MnO<sub>2</sub> or MnO<sub>2</sub>/graphene as active material with 20 wt% of acetylene black (conductive additive) and 10 wt% of binder polytetrafluoroethylene (PTFE). 70 mg of MnO<sub>2</sub> powder and 20 mg of acetylene black were firstly mixed and dispersed in ethanol by ultrasound for 30 min. Then the ink was dried at 80 °C for 4 h to get dark mixed powder and 10 mg of PTFE was added to get a paste with a few of ethanol. Then the paste was dried at 80 °C and a few of 1-methyl-2-pyrrolidinone (NMP) were added to get a syrup. The syrup was cold rolled into thick films. Pieces of film with 1–5 mg weight, typically 1 cm<sup>2</sup> in size, were then hot-pressed at 80 °C under 100 MPa on a stainless steel mesh. The prototype nickel ion battery with α-MnO<sub>2</sub> cathode, 1 mol L<sup>-1</sup> NiSO<sub>4</sub> aqueous electrolyte, a fiber paper separator and a nickel foam anode as shown in Figure S10. The nickel foam is used due to its larger surface area than plate.

Electrochemical tests were performed with Solartron 1480 electrochemical station and Land CT2001A equipment. The discharge capacity of the cell is calculated according to the formula:

$$C = \frac{I \cdot t}{m} \quad (4)$$

Where  $C$  is specific capacity (milliamper-hour per gram, mA·h g<sup>-1</sup>),  $I$  is the applied current (milliamper, mA),  $t$  is discharge time (hour, h), and  $m$  is the mass of the active material (gram). The energy density is calculated by the following equation:

$$E = C \cdot V \quad (5)$$

Where  $C$  is specific capacity (mA·h g<sup>-1</sup>) and  $V$  is the average voltage of battery. The average voltage of NIB and ZIB is 0.85 and 1.45 V.

The energy density of zinc ion battery (ZIB) and nickel ion battery (NIB) are listed in Table S2.

## References

- Roco, M. C. Nanotechnology for sustainability: Energy conversion, storage, and conversation in Nanotechnology Research Directions for Societal Needs in 2020: Retrospective and Outlook, Ch. 6, 268 (*Science Policy Reports*, 2011).
- Winter, M. & Brodd, R. J. What are batteries, fuel cells, and supercapacitors? *Chem. Rev.* **104**, 4245–4269 (2004).
- Patil, A. *et al.* Issue and challenges facing rechargeable thin film lithium batteries. *Mater. Res. Bull.* **43**, 1913–1942 (2008).
- Ji, X., Lee, K. T. & Nazar, L. F. A highly ordered nanostructured carbon-sulphur cathode for lithium-sulphur batteries. *Nature Mater.* **8**, 500–506 (2009).
- Peng, Z., Freunberger, S. A., Chen, Y. & Bruce, P. G. A reversible and higher-rate Li-O<sub>2</sub> battery. *Science* **337**, 563–566 (2012).
- Slater, M. D., Kim, D., Lee, E. & Johnson, C. S. Sodium-Ion Batteries. *Adv. Funct. Mater.* **23**, 947–958 (2013).
- Palomares, V. *et al.* Na-ion batteries, recent advances and present challenges to become low cost energy storage systems. *Energy Environ. Sci.* **5**, 5884–5901 (2012).
- Beck, F. & Ruetschi, P. Rechargeable batteries with aqueous electrolytes. *Electrochim. Acta* **45**, 2467–2482 (2000).
- Aurbach, D. *et al.* Prototype systems for rechargeable magnesium batteries. *Nature* **407**, 724–727 (2000).
- Rasul, S., Suzuki, S., Yamaguchi, S. & Miyayama, M. Synthesis and electrochemical behavior of hollandite MnO<sub>2</sub>/acetylene black composite cathode for secondary Mg-ion batteries. *Solid State Ionics* **225**, 542–546 (2012).
- Zhang, R. *et al.* α-MnO<sub>2</sub> as a cathode material for rechargeable Mg batteries. *Electrochem. Commun.* **23**, 110–113 (2012).
- Jayaprakash, N., Das, S. K. & Archer, L. A. The rechargeable aluminum-ion battery. *Chem. Commun.* **47**, 12610–12612 (2011).
- Tarascon, J. M. & Armand, M. Issues and challenges facing rechargeable lithium batteries. *Nature* **414**, 359–367 (2001).
- Wang, W. *et al.* A new cathode material for super-valent battery based on aluminium ion intercalation and deintercalation. *Sci. Rep.* **3**, 3383 (2013).
- Rani, J. V., Kanakaiah, V., Dadmal, T., Rao, M. S. & Bhavanarushi, S. Fluorinated Natural Graphite Cathode for Rechargeable Ionic Liquid Based Aluminum-Ion Battery. *J. Electrochem. Soc.* **160**, A1781–A1784 (2013).
- Liu, S. *et al.* Aluminum storage behavior of anatase TiO<sub>2</sub> nanotube arrays in aqueous solution for aluminum ion batteries. *Energy Environ. Sci.* **5**, 9743–9746 (2012).
- Singh, N., Arthur, T. S., Ling, C., Matsui, M. & Mizuno, F. A high energy-density tin anode for rechargeable magnesium-ion batteries. *Chem. Commun.* **49**, 149–151 (2013).
- Xu, C., Wei, C., Kang, F. & Guan, Z. Charge storage mechanism of manganese dioxide for capacitor application: Effect of the mild electrolytes containing alkaline and alkaline-earth metal cations. *J. Power Sources* **196**, 7854–7859 (2011).
- Xu, C., Du, H., Li, B., Kang, F. & Zeng, Y. Capacitive Behavior and Charge Storage Mechanism of Manganese Dioxide in Aqueous Solution Containing Bivalent Cations. *J. Electrochem. Soc.* **156**, A73–A78 (2009).
- Xu, C., Du, H., Li, B., Kang, F. & Zeng, Y. Reversible Insertion Properties of Zinc Ion into Manganese Dioxide and Its Application for Energy Storage. *Electrochem. Solid-State Lett.* **12**, A61–A65 (2009).
- Munaiah, Y., Raj, B. G. S., Kumar, T. P. & Ragupathy, P. Facile synthesis of hollow sphere amorphous MnO<sub>2</sub>: the formation mechanism, morphology and effect of a bivalent cation-containing electrolyte on its supercapacitive behavior. *J. Mater. Chem. A* **1**, 4300–4306 (2013).
- Nayak, P. K. & Munichandraiah, N. Reversible Insertion of a Trivalent Cation onto MnO<sub>2</sub> Leading to Enhanced Capacitance. *J. Electrochem. Soc.* **158**, A585–A591 (2011).
- Xu, C., Li, B., Du, H. & Kang, F. Energetic Zinc Ion Chemistry: The Rechargeable Zinc Ion Battery. *Angew. Chem. Int. Ed.* **51**, 933–935 (2012).

24. Khomeiko, V., Raymundo-Pinero, E. & Beguin, F. Optimisation of an asymmetric manganese oxide/activated carbon capacitor working at 2 V in aqueous medium. *J. Power Sources* **153**, 183–190 (2006).
25. Ling, C. & Mizuno, F. Capture Lithium in  $\alpha\text{-MnO}_2$ : Insights from First Principles. *Chem. Mater.* **24**, 3943–3951 (2012).
26. Trocoli, R. & La Mantia, F. An aqueous zinc-ion battery based on copper hexacyanoferrate. *ChemSusChem*. **8**, (3) 481–485 (2015).
27. Lee, B. *et al.* Electrochemically-induced reversible transition from the tunneled to layered polymorphs of manganese dioxide. *Scientific Reports*, **4**, 2014, doi: 10.1038/srep06066.
28. Zhang, B. H. *et al.* An aqueous rechargeable battery based on zinc anode and  $\text{Na}_{0.95}\text{MnO}_2$ . *Chem. Commun.* **50**, (10) 2109–2111, (2014).
29. Lee, J., Ju, J. B., Cho, W. I., Cho, B. W., Oh, S. H. Todorokite-type  $\text{MnO}_2$  as a zinc-ion intercalating material. **112**, 138–143, (2013).
30. Luo, J.-Y., Cui, W.-J., He, P. & Xia, Y.-Y. Raising the cycling stability of aqueous lithium-ion batteries by eliminating oxygen in the electrolyte. *Nature Chem.* **2**, 760–765 (2010).

## Acknowledgments

We would like to thank NSFC (No. 51102139) and Shenzhen Technical Plan Projects (No. JC201105201100A and JCYJ20130402145002425) for financial support. We also appreciate the financial support from Guangdong Province Innovation R&D Team Plan (2009010025).

## Author Contributions

C.X. conceived concept, wrote the manuscript, and performed the experiments. Y.C., C.X., S.S. and J.L. performed simulation. C.X., F.K. and D. S. revised the manuscript. All authors reviewed the manuscript.

## Additional Information

**Supplementary information** accompanies this paper at <http://www.nature.com/srep>

**Competing financial interests:** The authors declare no competing financial interests.

**How to cite this article:** Xu, C. *et al.* Secondary batteries with multivalent ions for energy storage. *Sci. Rep.* **5**, 14120; doi: 10.1038/srep14120 (2015).



This work is licensed under a Creative Commons Attribution 4.0 International License. The images or other third party material in this article are included in the article's Creative Commons license, unless indicated otherwise in the credit line; if the material is not included under the Creative Commons license, users will need to obtain permission from the license holder to reproduce the material. To view a copy of this license, visit <http://creativecommons.org/licenses/by/4.0/>